

Motion of ferrodark solitons in harmonically trapped superfluids: spin corrections and emergent quartic potentials exhibiting symmetry breaking

Jiangnan Biguo¹ and Xiaoquan Yu^{1,2,*}

¹Graduate School of China Academy of Engineering Physics, Beijing 100193, China

²Department of Physics, Centre for Quantum Science,
and Dodd-Walls Centre for Photonic and Quantum Technologies,
University of Otago, Dunedin 9016, New Zealand

We propose a framework for topological soliton dynamics in trapped spinor superfluids, decomposing the force acting on the soliton by the surrounding fluid into the buoyancy force and spin-corrections arising from the density depletion at soliton core and the coupling between the orbital motion and the spin mixing, respectively. For ferrodark solitons (FDSs) in spin-1 Bose-Einstein Condensates (BECs), the spin correction enables mapping the FDS motion in a harmonic trap to the atomic-mass particle dynamics in an emergent *quartic* potential. Initially placing a type-I FDS near the trap center, a single-sided oscillation happens, which maps to the particle moving around a local minimum of the emergent double-well potential. As the initial distance of a type-II FDS from the trap center increases, the motion exhibits three regimes: trap-centered harmonic and anharmonic, followed by single-sided oscillations. Correspondingly the emergent quartic potential undergoes symmetry breaking, transitioning from a single minimum to a double-well shape, where particle motion shifts from oscillating around the single minimum to crossing between two minima via the local maximum, then the motion around one of the two minima. In a hard-wall trap with linear potential, the FDS motion maps to a harmonic oscillator.

Introduction– Topological excitations associated with discrete symmetries, such as dark solitons, kinks and domain walls, exist in various systems and are of interest in many research areas [1–3]. In superfluids, their dynamics reveals rich properties of superfluidity in the non-linear regime. In a quasi-one-dimensional (1D) harmonically trapped system where the system size is much larger than the soliton width, the ratio between the dark soliton oscillation frequency and the trap frequency is $1/\sqrt{2}$ for Bose gases [4–6] and is approximately $1/\sqrt{3}$ for unitary Fermi gases [7, 8]. Such results can be obtained from the macroscopic equation of motion (EOM) $M_{\text{in}}d^2X/dt^2 = f_b$, where X is the soliton position, $f_b = \delta NdU/dX$ is the buoyancy force, $U(x)$ is the trap potential, $M_{\text{in}} = 2\delta\delta K/\partial V^2$ is the inertial mass, δK is the soliton energy, $V = dX/dt$ is the soliton velocity, and δN is the atom number deficiency due to the density depression at the core. However, the relation $\partial\delta K(\mu, V^2)/\partial\mu = \delta N$, an important step in the derivation from the energy conservation $d\delta K/dt = 0$, was shown invalid for magnetic solitons in a two-component BEC at finite V [9], indicating this traditional formulation only applies to small amplitude oscillations [10]. While a FDS [11–14] exhibits oscillations in a linear potential and the amplitude can be as large as the system size [12]. Hence to describe large amplitude soliton oscillations involving spin-degrees of freedom, an alternative formulation is demanded.

In this Letter, we develop a formalism capable of describing the spin-dependent soliton motion in a quasi-1D trapped spinor superfluid and establish a mapping between the soliton motion and the dynamics of a particle with the atomic mass M in an emergent potential. Distinct from the traditional description [5, 8], in our formu-

lation the soliton EOM reads $M_{\text{in}}d^2X/dt^2 = f = f_b + f_s$, where the total force f contains the buoyancy force f_b and the additional spin-correction f_s , clarifying the origin of the force acting on solitons in a trapped system. The spin-correction can be evaluated from the soliton energy explicitly and governs spin-dependent soliton motion while absent in scalar soliton like nonlinear waves. We consider FDSs [12] in a trapped spin-1 BEC and find that f_s and f_b have opposite signs for type-II FDSs and the total force f could vanish and change sign where $dU/dx \neq 0$, yields to non-trivial equilibrium positions of the soliton motion. At the transition point between type-I and type-II FDSs, both f_s and M_{in} diverge and change sign while f/M_{in} keeps finite and non-zero. The buoyancy force f_b remains finite and constant-sign. In a harmonic trap and a linear potential, the FDS motion maps to a *quartic* oscillator exhibiting symmetry breaking and a harmonic oscillator, respectively. Using this mapping, the oscillation frequencies are obtained analytically utilizing exact FDSs solutions [12].

Systems– The mean-field Hamiltonian density of a quasi-1D spin-1 BEC is [15–19]:

$$H = \frac{\hbar^2|\partial_x\psi|^2}{2M} + \frac{g_n}{2}n^2 + \frac{g_s}{2}|\mathbf{F}|^2 + U(x)n + q\psi^\dagger\hat{S}_z^2\psi, \quad (1)$$

where $\psi = (\psi_{-1}, \psi_0, \psi_{+1})^T$ with components $\psi_{m=-1,0,1}$ denoting the amplitudes of magnetic sublevels, M is the atomic mass, $n = \psi^\dagger\psi = \sum_m |\psi_m|^2 = \sum_m n_m$ is the total number density, n_m is the component density, the magnetization $\mathbf{F} = \psi^\dagger\mathbf{S}\psi$ serves the order parameter associated with the SO(3) symmetry, $\mathbf{S} = (S_x, S_y, S_z)$, $S_{j=x,y,z}$ are spin-1 matrices, $U(x)$ is the spin-independent potential, and $g_n > 0$ and g_s are the density and spin-

dependent interaction strength, respectively. The external magnetic field is along the z -axis and q represents the quadratic Zeeman energy. The dynamics at zero temperature is governed by the spin-1 Gross-Pitaevskii equations (GPEs): $\partial\psi/\partial t = \delta H/\delta(i\hbar\psi^\dagger)$. For the ferromagnetic coupling ($g_s < 0$) and $0 < \tilde{q} \equiv -q/(2g_s n_b) < 1$, the uniform ground state is the easy-plane phase under the constraint $F_z = 0$ and is characterized by non-vanishing transverse magnetization $F_\perp \equiv F_x + iF_y$ [18, 19], where n_b denotes the total number density.

Ferrodark solitons– In the easy plane phase, ferrodark solitons (FDSs) are \mathbb{Z}_2 topological defects in the spin order (magnetic kinks) with positive (type-I) and negative (type-II) inertial mass. At $g_s = -g_n/2$, the exact solutions are available and the transverse magnetization read [12]: $F_\perp^{I,II}(x,t) = \sqrt{n_b^2 - q^2/g_n^2} \tanh[(x - Vt)/\ell^{I,II}]$, where the width $\ell^{I,II} = \sqrt{2\hbar^2/M(g_n n_b - MV^2 \mp Q)}$, the minus (plus) sign in front of Q specifies type-I (II) FDS and $Q = \sqrt{M^2 V^4 + q^2 - 2g_n n_b M V^2}$. When $Q = 0$, the speed limit $V = C_{\text{FDS}} = \sqrt{g_n n_b/M} \sqrt{1 - \sqrt{1 - (q/g_n n_b)^2}}$ is reached and the transition between two types occurs [12]. The soliton energy $\delta K = H[\psi_s] + \mu\delta N - H[\psi_g] = K_s - K_g$, where $K_s = \int dx (H[\psi_s] - \mu n)$, $K_g = \int dx (H[\psi_g] - \mu n_b)$, ψ_s is the soliton wavefunction, $\delta N = \int dx (n_b - n_s)$ is the depleted atom number, ψ_g is the ground state wavefunction, and $\mu = (g_n + g_s)n_b + q/2$ is the chemical potential. For FDSs, the total density $n^{I,II}$ shows a dip (but does not vanish) at the core and the energy is

$$\delta K^{I,II}(n_b, \mu, V^2) = \frac{4\hbar^4}{3g_n M^2 (\ell^{I,II})^3} - \left(\frac{g_n n_b + q}{2} - \mu \right) \delta N^{I,II}, \quad (2)$$

where $\delta N^{I,II} = 2\hbar^2/g_n M \ell^{I,II}$ [20].

Reformulation of soliton dynamics and spin corrections– To incorporate the effect of spin mixing, here we propose a refined theory of soliton motion in a trapped superfluid. Comparing to the original theory developed in Refs. [5, 8], where the excitation energy for the homogeneous system is parameterized by μ and V^2 , the key difference of our formulation is parameterizing the excitation energy $\delta K(n_b, \mu, V^2)$ using n_b , μ and V^2 with μ appearing only in the term $\mu\delta N$. Then within the local density approximation, the soliton excitation energy in a trapped BEC can be obtained by taking the following substitution into $\delta K(n_b, \mu, V^2)$:

$$\mu \rightarrow \mu[X(t)] = \mu_N - U[X(t)], \quad (3)$$

$$n_b \rightarrow n_b[X(t)], \quad V \rightarrow \frac{dX(t)}{dt}, \quad (4)$$

where $X(t)$ is the soliton position, $n_b(x)$ is ground state density profile for the trapped system which can be ob-

tained within Thomas-Fermi (TM) approximation [1], and μ_N is determined by the total atom number N [21].

Apparently $\delta K\{n_b[X(t)], \mu[X(t)], V(t)^2\}$ is function of $X(t)$ and $V(t)$ and we introduce $\delta\hat{K}[X(t), V^2(t)] \equiv \delta K\{n_b[X(t)], \mu[X(t)], V(t)^2\}$. The energy conservation law $d\delta\hat{K}[X(t), V^2(t)]/dt = (\partial\delta\hat{K}/\partial X)(dX/dt) + (\partial\delta\hat{K}/\partial V^2)(dV^2/dt) = 0$ gives rise to

$$M_{\text{in}} \frac{d^2 X}{dt^2} = f = f_b + f_s, \quad (5)$$

where $M_{\text{in}} \equiv 2\partial\delta\hat{K}/\partial V^2$ is the soliton inertial mass, and the total force acting on the soliton $f \equiv -\partial\delta\hat{K}/\partial X$ is decomposed into two parts:

$$f_b = -\frac{\partial\delta K}{\partial\mu(X)} \frac{\partial\mu(X)}{\partial X}, \quad f_s = -\frac{\partial\delta K}{\partial n_b(X)} \frac{\partial n_b(X)}{\partial X}. \quad (6)$$

Here $\partial\delta K/\partial\mu = \int dx [n_b(x) - n_s(x)] = \delta N$ is valid for any velocity and $f_b = \delta N \partial U(X)/\partial X$ is the buoyancy force. We denote the additional force f_s as the *spin correction*. For scalar dark solitons and dark-dark-dark (DDD) solitons in the easy plane phase [22], f_s vanishes while becomes non-trivial for FDSs:

$$f_s^{I,II} = -\frac{\partial\delta K^{I,II}}{\partial n_b(X)} \Big|_{n_b=n_b^{\text{TF}}} \frac{\partial n_b(X)}{\partial X} = \mp \frac{\hbar^2 V^2}{Q \ell^{I,II}} \frac{\partial n_b(X)}{\partial X}, \quad (7)$$

which is evaluated at the TM density [22] and here the minus (plus) sign corresponds to type-I (II) FDS. Then the EOM of a FDS in a trapped spin-1 BEC reads $M_{\text{in}}^{I,II} d^2 X/dt^2 = f^{I,II} = f_b^{I,II} + f_s^{I,II}$, where

$$M_{\text{in}}^{I,II} = 2 \frac{\partial\delta\hat{K}^{I,II}}{\partial V^2} \Big|_{n_b=n_b^{\text{TF}}} = \pm \frac{4\hbar^4}{g_n M Q (\ell^{I,II})^3}, \quad (8)$$

$$f_b^{I,II} = -\frac{\partial\delta K^{I,II}}{\partial\mu} \Big|_{n_b=n_b^{\text{TF}}} \frac{\partial\mu(X)}{\partial X} = -\frac{2\hbar^2}{g_n M \ell^{I,II}} \frac{\partial\mu(X)}{\partial X}, \quad (9)$$

and the plus (minus) sign in Eq. (8) corresponds to type-I (II) FDS.

Equilibrium positions and the maximum speed– The equilibrium positions occur where $a = f/M_{\text{in}} = 0$. For FDSs, the total force is $f^{I,II} = (2\hbar^2/g_n M \ell^{I,II})(1 \pm MV^2/Q)\partial U(X)/\partial X$. When approaching the type transition point $Q \rightarrow 0$, both $M_{\text{in}}^{I,II}$ and $f_s^{I,II}$ diverge (f_b keeps finite) while the ratio $f^{I,II}/M_{\text{in}}^{I,II}$ remains finite and nonzero [Eqs. (7) and (8)]. Then the equilibrium positions do not locate at where M_{in} diverges ($Q = 0$) but locate where the force vanishes (with sign change) happening either when $\partial U/\partial X = 0$ or when $1 - MV^2/Q = 0$ while $\partial U/\partial X \neq 0$ (for type-II FDSs). As it follows the locations of the maximum speed ($f^{\text{II}} = 0$) and reaching the local speed limit ($Q = 0$) in the motion of a FDS do not coincide. While this maximum speed value is still less than the local speed limit $C_{\text{FDS}}[n_b(x)]$ [23]. This scenario is illustrated explicitly in the case of a hard-wall confined

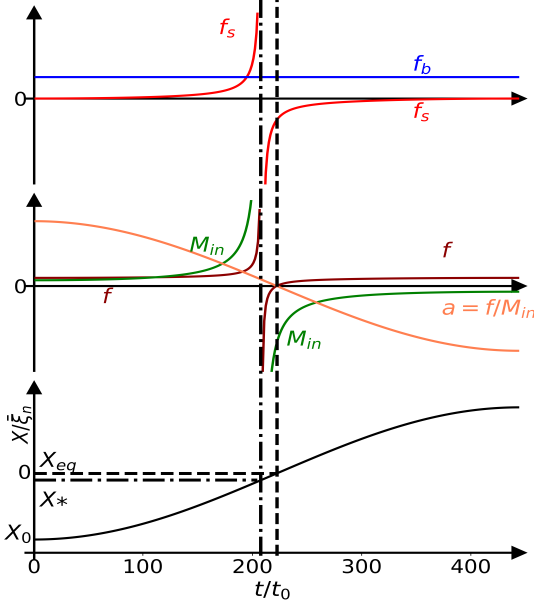


FIG. 1. Evolution of the inertial mass M_{in} (green), the constant buoyancy force f_b (blue), the spin correction f_s (red), the total force f (dark red), and the trajectory (black solid) during a half period of the oscillation in a linear potential with initially placing a type-I FDS at X_0 , evaluated using Eqs. (7) (8) and (9). When crossing the type transition point $X_* = \mu_N/k - \sqrt{(\mu_N/k - X_0 - q/k)^2 + q^2/4k^2} - q/2k$ (guided by the dash-dotted line), M_{in} , f_s and f diverge and change sign. The acceleration a (orange) keeps sign before reaching the nearby equilibrium point $X_{eq} = X_0 + q/2k > X_*$ (guided by the dash line), where the total force f vanishes and changes sign again. Here $X_0 = -10\tilde{\xi}_n$, $\tilde{q} = -q/2g_s\bar{n}_b = 0.2$, $\mu_N = 0.6g_n\bar{n}_b$, $k = 0.01g_n\bar{n}_b/\tilde{\xi}_n$ (for the parameters chosen, $X_{eq} = 0$), $\tilde{\xi}_n = \sqrt{\hbar^2/Mg_n\bar{n}_b}$, $t_0 = \hbar/g_n\bar{n}_b$, and \bar{n}_b is the average density.

system subjected to a linear potential $U(x) = kx$ (Fig. 1).

Emergent harmonic oscillators – The FDS motion in a trapped spin-1 BEC involves complex evolution of the inertial mass and the forces (Fig. 1). On the other hand, remarkably, the EOM of a FDS [Eq. (5)] maps to a dynamical system of a particle with the atomic mass: $dX/dt = \partial\tilde{H}/\partial P$, $dP/dt = -\partial\tilde{H}/\partial X$, where $\tilde{H} = P^2/2M + \tilde{U}(X)$, $P = M dX/dt$ and the emergent potential

$$\tilde{U}(X) = -\frac{2\mu_N - 4E_0^{I,II} - q}{4E_0^{I,II}}U(X) + \frac{1}{4E_0^{I,II}}U(X)^2. \quad (10)$$

Here $E_0^{I,II} = \hbar^2/2M(\ell^{I,II})^2 = \hbar^2/2M[\ell^{I,II}(X_0, V_0)]^2$ is determined by the initial position X_0 and the initial velocity V_0 of the soliton and serves an energy unit. The FDS motion in a linear potential described in Fig. 1 maps to a

harmonic oscillator and Eq. (10) becomes

$$\tilde{U}(X) = \frac{1}{2}M\omega_0^2(X - X_{eq})^2 - \frac{1}{2}M\omega_0^2X_{eq}^2, \quad (11)$$

where the equilibrium position $X_{eq} = (2\mu_N - 4E_0^{I,II} - q)/2k = X_0 \pm q/2k$ [plus (minus) sign specifies the type-I (II) FDS initially placed](coincide with condition $f^{II} = 0$). The X_0 -dependent oscillation frequency and the X_0 -independent amplitude A read [24]

$$\omega_0 = \frac{|k|}{\sqrt{2ME_0^{I,II}}} \quad \text{and} \quad A = \frac{q}{2|k|}. \quad (12)$$

Emergent quartic oscillators and symmetry breaking– For a harmonic potential $U(X) = M\omega^2X^2/2$,

$$\tilde{U}(X) = -\frac{1}{2}bM\omega^2X^2 + \frac{\lambda}{4}X^4, \quad (13)$$

where $b = (2\mu_N - 4E_0^{I,II} - q)/4E_0^{I,II}$ and $\lambda = M^2\omega^4/4E_0^{I,II} > 0$. Hence the FDS motion in a harmonically trapped spin-1 BEC maps to a *quartic* oscillator, a result of the combination of the buoyancy force and the spin correction[25].

For a stationary ($V_0 = 0$) type-I FDS initially placed at X_0 near the origin, since $M_{in}^I > 0$ and the force f^I points outwards, it starts to move towards to the condensate boundary and later undergoes a type transition, leading to a periodic motion on the one side of the harmonic trap [Fig. 2(a1)] with the equilibrium position located where the spin-correction balances the buoyancy force ($1 - MV^2/Q = 0$). Since $b = [2U(X_0) + q]/4E_0^I > 0$, $\tilde{U}(X)$ is a *double-well* potential and the two minima locate at $X = X_{eq}^I = \pm\sqrt{X_0^2 + q/M\omega^2}$ with $|X_{eq}^I| > X_0$ [26]. This motion then maps to a particle oscillating around a local minima of the emergent potential [Fig. 2(b1)]. To avoid reaching the phase boundary separating the easy plane phase from the polar state, the initial position of the FDS should satisfies $|X_0| < \sqrt{(2\mu_N - 4q)/(M\omega^2)}$ [27]. When the oscillation amplitude is small, expanding \tilde{U} around X_{eq}^I we obtain $\tilde{U} = \tilde{U}''(X_{eq}^I)(X - X_{eq}^I)^2/2$ and the oscillation frequency is

$$\omega^I = \sqrt{\frac{\tilde{U}''(X_{eq}^I)}{M}} = \omega \sqrt{\frac{2[2U(X_0) + q]}{g_n n_b^{TF}(X_0) - q}}. \quad (14)$$

Starting with a type-II FDS, three distinct trajectories are found: i) Initially placed at X_0 near the origin, the type-II FDS oscillates harmonically around the trap center [Fig. 2(a2)]. Since $b = [2U(X_0) - q]/4E_0^{II} < 0$ for sufficiently small $|X_0|$, the emergent particle potential $\tilde{U}(X)$ exhibits a single minimum [Fig. 2(b2)]. For small amplitude oscillation ($|bM\omega^2| \gg \lambda X_0^2$), the oscillation frequency is obtained by neglecting the quartic term [28]:

$$\omega_s^{II} = \sqrt{\frac{\tilde{U}''(0)}{M}} = \omega \sqrt{\frac{q}{g_n n_b^{TF}(0) + q}}, \quad (15)$$

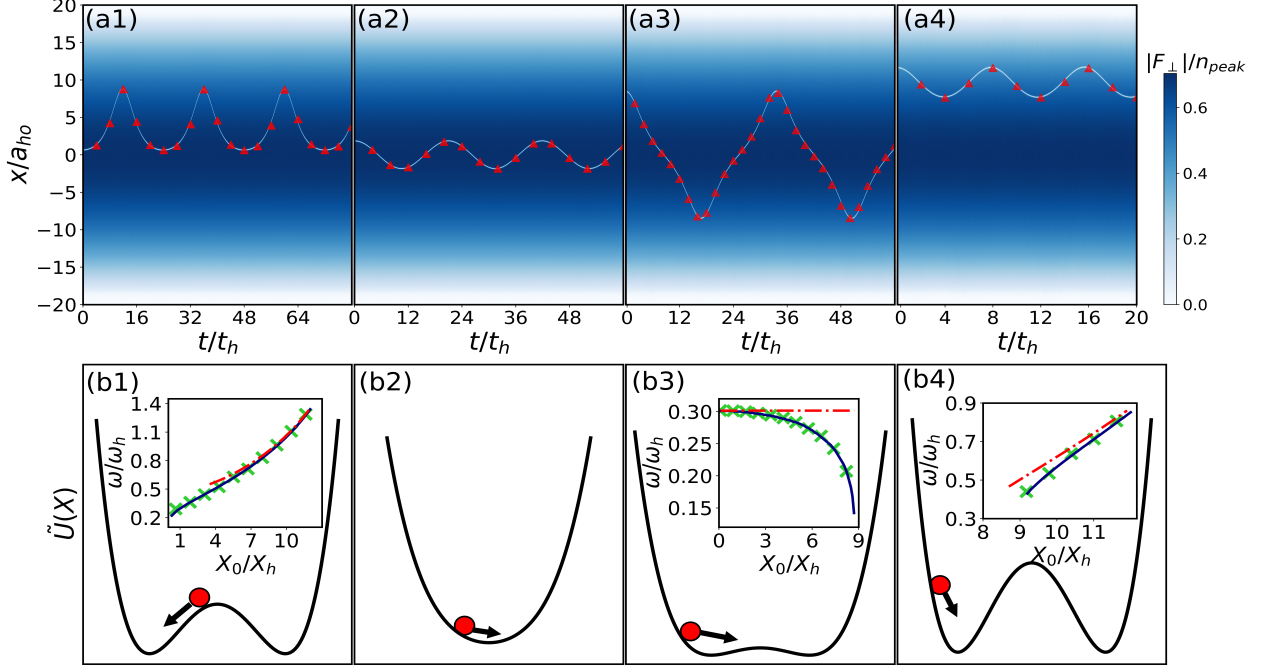


FIG. 2. FDS dynamics in a harmonically trapped spin-1 BEC: a FDS core trajectory evolution[(a1)-(a4)] [spin-1 GPE simulations (lines); macroscopic soliton EOM Eq. (5) (markers)] and the corresponding emergent particle quartic potential $\tilde{U}(X)$ [(b1)-(b4)](schematic). Here $g_s/g_n = -1/2$, $\tilde{q} = -q/2g_s n_{\text{peak}} = 0.1$, $\mu_N = 201.2\hbar\omega_h$, $a_{\text{ho}} = \sqrt{\hbar/(M\omega_h)}$, $t_h = 1/\omega_h$ and ω_h is the trap frequency. (a1): a type-I FDS is initially placed near the trap center, it drifts away from the trap center and then returns, exhibiting single-sided oscillations, mapping to a particle rolling down from the local maximum and then oscillating around a local minima of an emergent double-well potential [(b1)]; (a2)-(a4): when imprinting a type-II FDS, the motion depends on the initial distance to the trap center: (a2) slightly away: harmonic oscillation of a type-II FDS near the trap center, mapping to particle oscillations around the single minima of the emergent quartic potential [(b2)]; (a3) further away: anharmonic oscillation centered at the trap origin, mapping to a particle going around the local maximum of the symmetry breaking double-wall potential [(b3)]; (a4) far enough: single-sided oscillations [inverse process of (a1)], mapping to a particle moving around a local minimum [(b4)]. Insets in (b1)(b3) and (b4) show the initial position dependence of oscillation frequencies: analytical predictions for small amplitude (red dash-dotted line) [Eqs. (14), (15) and (16)] and for large amplitude oscillations (black solid line) evaluated via $\omega = 2\pi/|2 \int_{X_0}^{X_{\text{end}}} 1/V(X)dX|$, and spin-1 GPEs simulations (markers).

which is independent of X_0 and in this case the spin-correction plays little role. ii) When $|X_0| > X_0^c$ with $X_0^c = \sqrt{q/M\omega^2}$ determined by $b(X_0^c) = 0$, $b > 0$ and $\tilde{U}(X)$ undergoes a symmetry-breaking transition and becomes a *double-well* potential with two minima located at $X = X_{\text{eq}}^{\text{II}} = \pm \sqrt{X_0^2 - q/M\omega^2}$ ($|X_{\text{eq}}^{\text{II}}| < X_0$) [balance between f_b and f_s^{II} : $1 - MV^2/Q = 0$]. When $X_0^c < |X_0| < \sqrt{2}X_0^c$, $\tilde{U}(X_0) > \tilde{U}(0) = 0$, the mapped particle motion is oscillatory around the origin while the trajectory crosses the maximum and the two minima of the potential $\tilde{U}(X)$ [Fig. 2(b3)]. This corresponds to a periodic motion of a FDS around the trap center while far from being harmonic [Fig. 2(a3)]. iii) For sufficiently large $|X_0|$, i.e., $|X_0| > \sqrt{2}X_0^c$ [29], $\tilde{U}(X_0) < \tilde{U}(0) = 0$, the oscillation around a local minimum $X = X_{\text{eq}}^{\text{II}}$ happens [Fig. 2(b4)] and this corresponds to a periodic motion of a FDS on the one side of the harmonic trap [Fig. 2(a4)]. Around

$X_{\text{eq}}^{\text{II}}$, $\tilde{U} \approx \tilde{U}''(X_{\text{eq}}^{\text{II}})(X - X_{\text{eq}}^{\text{II}})^2/2$ and the oscillation frequency for small amplitudes reads

$$\omega^{\text{II}} = \sqrt{\frac{\tilde{U}''(X_{\text{eq}}^{\text{II}})}{M}} = \omega \sqrt{\frac{2[2U(X_0) - q]}{g_n n_b^{\text{TF}}(X_0) + q}}. \quad (16)$$

By increasing $|X_0|$, the emergent particle potential undergoes a symmetry breaking transition, exhibiting a single minimum when $|X_0| < X_0^c$ and two local minima when $|X_0| > X_0^c$, where the critical value X_0^c is given by flatness condition of the emergent quartic potential $b = 0$. This condition corresponds to the type-II FDS transferring to type-I FDS right at the trap center. Indeed the onset condition for the type transition is $E_0^{\text{II}}(X_0, 0) = E_0^{\text{II}}(0, C_{\text{FDS}}[n_b^{\text{TF}}(0)])$ leading to $|X_0| = \sqrt{2\mu_N(1 - \sqrt{1 - q/\mu_N})}/M\omega^2 \approx X_0^c$ for $q/\mu_N \ll 1$ which is fulfilled within the requirement of the TM approxima-

tion. Hence in the broken symmetry case [ii) and iii)], the FDS motion involves the type transition [12].

Conclusion—We formulate a theory of describing spin-dependent soliton motion in a system confined by an external potential, in which the total force acting on the soliton is decomposed into the buoyancy force and the spin correction. The interplay between the inertial mass, the buoyancy force and the spin correction leads to single-sided and trap-centered oscillations of ferrodark solitons in a harmonically trapped spin-1 BEC, mapping to an atomic-mass particle moving in an emergent quartic potential. Oscillation frequencies of ferrodark solitons involving type transitions are obtained analytically within this mapping which are otherwise challenging to calculate. Our formulation is applicable to various non-linear waves in trapped multi-component superfluids [30–37]. For magnetic solitons in trapped two-component BECs, our approach gives results [22] consistent with what reported in Ref. [9] which were obtained from a different perspective. Experimental investigations of rich dynamics of ferrodark solitons in trapped systems are also within the scope of current ultracold-gas experiments [32, 33, 38–43].

ACKNOWLEDGMENT

We thank Y. Bai, R. Han, P. B. Blakie for useful discussions. X.Y. acknowledges support from the National Natural Science Foundation of China (Grant No. 12175215, Grant No. 12475041), the National Key Research and Development Program of China (Grant No. 2022YFA 1405300) and NSAF (Grant No. U2330401).

* xqyu@g scaep.ac.cn

- [1] L. Pitaevskii and S. Stringari, *Bose-Einstein condensation and superfluidity*, Vol. 164 (Oxford University Press, 2016).
- [2] P. M. Chaikin, T. C. Lubensky, and T. A. Witten, *Principles of condensed matter physics*, Vol. 10 (Cambridge university press Cambridge, 1995).
- [3] T. Vachaspati, *Kinks and domain walls: An introduction to classical and quantum solitons* (Cambridge University Press, 2007).
- [4] T. Busch and J. R. Anglin, *Phys. Rev. Lett.* **84**, 2298 (2000).
- [5] V. V. Konotop and L. Pitaevskii, *Phys. Rev. Lett.* **93**, 240403 (2004).
- [6] A. Weller, J. P. Ronzheimer, C. Gross, J. Esteve, M. K. Oberthaler, D. J. Frantzeskakis, G. Theoharis, and P. G. Kevrekidis, *Phys. Rev. Lett.* **101**, 130401 (2008).
- [7] R. Liao and J. Brand, *Phys. Rev. A* **83**, 041604 (2011).
- [8] R. G. Scott, F. Dalfovo, L. P. Pitaevskii, and S. Stringari, *Phys. Rev. Lett.* **106**, 185301 (2011).
- [9] L. P. Pitaevskii, *Physics-Usp ekhi* **59**, 1028 (2016).
- [10] It works accidentally for dark solitons in scalar BECs at finite velocities [9, 22].
- [11] X. Yu and P. B. Blakie, *Phys. Rev. Res.* **3**, 023043 (2021).
- [12] X. Yu and P. B. Blakie, *Phys. Rev. Lett.* **128**, 125301 (2022).
- [13] X. Yu and P. B. Blakie, *Phys. Rev. Res.* **4**, 033056 (2022).
- [14] X. Yu and P. B. Blakie, *Phys. Rev. A* **110**, L061303 (2024).
- [15] T.-L. Ho, *Phys. Rev. Lett.* **81**, 742 (1998).
- [16] T. Ohmi and K. Machida, *Journal of the Physical Society of Japan* **67**, 1822 (1998).
- [17] L.E.Sadler, J. Higbie, S.R.Leslie, M.Vengalattore, and D.M.Stamper-Kurn, *Nature* **443**, 312 (2006).
- [18] D. M. Stamper-Kurn and M. Ueda, *Rev. Mod. Phys.* **85**, 1191 (2013).
- [19] Y. Kawaguchi and M. Ueda, *Physics Reports* **520**, 253 (2012).
- [20] The last term in Eq. (2) vanishes for a homogeneous system while here we keep it for the purpose of studying the soliton dynamics in a trapped system.
- [21] This method works well when the total atom number is much larger than that of soliton depletion and the width of soliton is much smaller than that of the condensate such that a stable background and a propagating soliton can be distinguished [44]. In this work, such conditions are assumed to be fulfilled.
- [22] See Supplemental Material for details.
- [23] $V/C_{\text{FDS}}[n_b(X)]$, i.e., measuring the velocity in terms of the local speed limit, reaches the maximum value 1 where the type transition happens [12]. Since the type transition point and the equilibrium point are very close to each other for feasible parameters, in numerical simulations the distinction between the two positions may be blurred by numerical errors [12].
- [24] Their q dependence is tested against numerical simulations and excellent agreements are found [22].
- [25] For scalar dark solitons and DDD solitons, where the spin corrections vanish, the emergent potential is still harmonic: $\tilde{U}(X) = (\omega/\sqrt{2})^2 MX^2/2$ [22].
- [26] Hence for $X_0 \neq 0$, there is no stationary position.
- [27] The oscillation occurs around one of the two minima $X = |X_{\text{eq}}^1|$ (or between X_0 and X_0^b), where $\tilde{U}(X_0^b) = \tilde{U}(X_0)$ and $X_0^b = \pm\sqrt{X_0^2 + 2q/M\omega^2}$. Let us denote x_b as the phase boundary separating the easy plane phase from the the polar state [22]. To avoid a FDS hitting on the phase boundary, we have $|X_0^b| < x_b$, which gives rise to $|X_0| < \sqrt{(2\mu_N - 4q)/(M\omega^2)}$.
- [28] In this small amplitude oscillation $\omega_s^{\text{II}} = \omega\sqrt{M_p^{\text{II}}/M_{\text{in}}^{\text{II}}}\Big|_{v=0}$, where $M_p \equiv -M\partial\delta K/\partial\mu$ is referred to as the physical mass.
- [29] Note that $|X_0| < x_b$ has to be satisfied, where x_b is the phase boundary separating the easy-plane phase from the polar phase [22].
- [30] C. Qu, L. P. Pitaevskii, and S. Stringari, *Phys. Rev. Lett.* **116**, 160402 (2016).
- [31] L.-C. Zhao, W. Wang, Q. Tang, Z.-Y. Yang, W.-L. Yang, and J. Liu, *Phys. Rev. A* **101**, 043621 (2020).
- [32] X. Chai, D. Lao, K. Fujimoto, R. Hamazaki, M. Ueda, and C. Raman, *Phys. Rev. Lett.* **125**, 030402 (2020).

- [33] A. Farolfi, D. Trypogeorgos, C. Mordini, G. Lamporesi, and G. Ferrari, *Phys. Rev. Lett.* **125**, 030401 (2020).
- [34] X. Chai, L. You, and C. Raman, *Phys. Rev. A* **105**, 013313 (2022).
- [35] W. Zhang, O. E. Müstecaplıoğlu, and L. You, *Phys. Rev. A* **75**, 043601 (2007).
- [36] S. Bresolin, A. Roy, G. Ferrari, A. Recati, and N. Pavloff, *Phys. Rev. Lett.* **130**, 220403 (2023).
- [37] L.-Z. Meng, S.-W. Guan, and L.-C. Zhao, *Phys. Rev. A* **105**, 013303 (2022).
- [38] L. Chomaz, L. Corman, T. Bienaimé, R. Desbuquois, C. Weitenberg, S. Nascimbène, J. Beugnon, and J. Dalibard, *Nat. Commun.* **6** (2015).
- [39] G. Gauthier, I. Lenton, N. M. Parry, M. Baker, M. J. Davis, H. Rubinsztein-Dunlop, and T. W. Neely, *Optica* **3**, 1136 (2016).
- [40] G. Semeghini, G. Ferioli, L. Masi, C. Mazzinghi, L. Wolswijk, F. Minardi, M. Modugno, G. Modugno, M. Inguscio, and M. Fattori, *Phys. Rev. Lett.* **120**, 235301 (2018).
- [41] J. M. Higbie, L. E. Sadler, S. Inouye, A. P. Chikkatur, S. R. Leslie, K. L. Moore, V. Savalli, and D. M. Stamper-Kurn, *Phys. Rev. Lett.* **95**, 050401 (2005).
- [42] S. Huh, K. Kim, K. Kwon, and J.-y. Choi, *Phys. Rev. Research* **2**, 033471 (2020).
- [43] M. Prüfer, D. Spitz, S. Lannig, H. Strobel, J. Berges, and M. K. Oberthaler, *Nature Physics* (2022).
- [44] V. A. Brazhnyi and V. V. Konotop, *Phys. Rev. A* **68**, 043613 (2003).
- [45] M. Matuszewski, *Phys. Rev. A* **82**, 053630 (2010).
- [46] W. Bao and F. Y. Lim, *SIAM J. Sci. Comput.* **30**, 1925 (2008).
- [47] G. C. Katsimiga, S. I. Mistakidis, P. Schmelcher, and P. G. Kevrekidis, *New J. Phys.* **23**, 013015 (2021).

Supplemental Material for “Motion of ferrodark solitons in harmonically trapped superfluids: spin corrections and emergent quartic potentials exhibiting symmetry breaking”

This Supplemental Material includes the derivation Thomas-Fermi approximation in spin-1 BECs, detailed calculations of spin corrections for scalar dark solitons and dark-dark-dark solitons in spin-1 BECs and other necessary materials for supporting the main results presented in the main manuscript.

THOMAS-FERMI APPROXIMATION IN SPIN-1 BECS

In the easy-plane phase the ground state component densities are $n_{\pm 1}^b = (1 - \tilde{q})n_b/4$ and $n_0^b = n_b(1 + \tilde{q})/2$, where n_b is the total number density. In the presence of a harmonic trap $U(x) = M\omega^2 x^2/2$, when the harmonic length $a_{ho} = \sqrt{\hbar/(M\omega)}$ is much larger than the spin healing length $\xi_s = \hbar/\sqrt{M|g_s|n_b(0)}$, or equivalently $\omega\hbar \ll |g_s|n_b(0)$, where ω is the trap frequency, the ground state wavefunction can be obtained by neglecting the kinetic term in the Gross-Pitaevskii equation [1, 45], which were referred to as the Thomas-Fermi approximation.

In the easy-plane phase, within this Thomas-Fermi approximation, the component densities read

$$n_{\text{TF}}^{\pm 1}(x) = \frac{\mu_N - U(x)}{4(g_n + g_s)} + \frac{g_n q}{8g_s(g_n + g_s)}, \quad (\text{S1})$$

$$n_{\text{TF}}^0(x) = \frac{\mu_N - U(x)}{2(g_n + g_s)} - \frac{(g_n + 2g_s)q}{4g_s(g_n + g_s)}, \quad (\text{S2})$$

and the total number density reads

$$n_{\text{TF}}^b(x) = n_{\text{TF}}^{+1} + n_{\text{TF}}^{-1} + n_{\text{TF}}^0 = \frac{2\mu_N - 2U(x) - q}{2(g_n + g_s)}, \quad (\text{S3})$$

where the chemical potential μ_N is fixed by the normalization condition $\int dx n_{\text{TF}}^b(x) = N$. The condensate size x_s is given by $n_{\text{TF}}^b(x_s) = 0$. A comparison between the Thomas-Fermi densities [Eqs. (S1) and (S2)] and numerical results which are obtained using the gradient flow method [46] is shown in Fig. S1. It is important to note that on the tails of the condensate, the density is low and the condition $0 < q < -2g_s n_{\text{TF}}^b(x)$ may not be satisfied for given quadratic Zeeman energy q . For a harmonic trap, the phase boundaries $\pm x_b$ are determined by $q = -2g_s n_{\text{TF}}^b(x_b)$ and we have $x_b = \sqrt{(2\mu_N g_s + g_n q)/(g_s M \omega^2)}$. For $x_b < |x| < x_s$, the system is in the polar state [18, 19] and consistently we have $n_{\text{TF}}^{\pm 1}(|x| \geq x_b) = 0$. In the following we focus on the region $|x| < x_b$ where $n_{\text{TF}}^{\pm 1}(x) > 0$ and the system is in the easy-plane phase. For a hard-wall trapped quasi-1D spin-1 BEC subjected to a linear potential $U(x) = kx$, the TF density in the bulk is

$$n_{\text{TF}}^b(x) = \frac{2\mu - 2kx - q}{2(g_n + g_s)}. \quad (\text{S4})$$

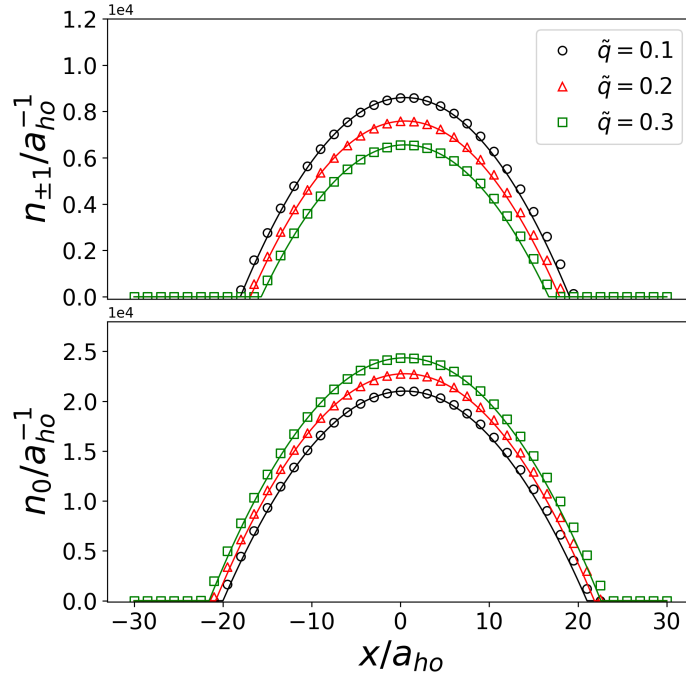


FIG. S1. Comparison of three component densities for a spin-1 BEC confined by a harmonic trap $U(x) = M\omega^2 x^2/2$ between the Thomas-Fermi approximation (solid lines) given by Eqs. (S1) and (S2) and numerical results obtained using the gradient flow method [46] (markers). Here $a_{ho} = \sqrt{\hbar/M\omega}$, $g_s/g_n = -1/2$, the total particle number $N = 10^6$, $\tilde{q} = -q/2g_s n_{\text{peak}} = 0.1, 0.2, 0.3$, and n_{peak} is the total density at the trap center $x = 0$.

In the main manuscript we only consider the situation where the Thomas-Fermi condition is fulfilled.

SPIN-CORRECTIONS OF SCALAR DARK SOLITONS AND DARK-DARK-DARK SOLITONS

In this section we show that for dark solitons in scalar BECs and dark-dark-dark solitons in spin-1 BECs the spin corrections vanish.

The soliton energy for a dark soliton in scalar BECs reads

$$\delta K_{\text{scalar}} = \frac{2\hbar \sqrt{\frac{gn_b(X)}{M} - V^2} [3\mu(X) - gn_b(X) - 2MV^2]}{3g}, \quad (\text{S5})$$

where g is the interaction strength.

Following Eq. (6) in the main manuscript, the spin correction for the scalar dark soliton is

$$f_s = \frac{\partial \delta K_{\text{scalar}}}{\partial n_b(X)} = \frac{\hbar [\mu(X) - gn_b(X)]}{M \sqrt{\frac{gn(X)}{M} - V^2}} \quad (\text{S6})$$

and it vanishes when taking the Thomas-Fermi density profile $n_b(x) = [\mu_N - U(x)]/g$.

Hence the equation of motion for a scalar dark soliton is

$$M_{\text{in}} \frac{d^2 X}{dt^2} = f_b, \quad (\text{S7})$$

where

$$M_{\text{in}} = 2 \left. \frac{\partial \delta K_{\text{scalar}}}{\partial V^2} \right|_{n_b=n^{\text{TF}}} = -\frac{4\hbar M}{g} \sqrt{\frac{gn_b(X)}{M} - V^2}, \quad (\text{S8})$$

and

$$f_b = -\left. \frac{\partial \delta K_{\text{scalar}}}{\partial \mu(X)} \frac{\partial \mu(X)}{\partial X} \right|_{n_b=n^{\text{TF}}} = \frac{2\hbar}{g} \sqrt{\frac{gn_b(X)}{M} - V^2} \frac{\partial U(X)}{\partial X}. \quad (\text{S9})$$

In the easy-plane phase, there exist stationary topological defects in the density superfluid order associated with the U(1) symmetry which are analogous to dark solitons in scalar BECs [1] and are referred to as dark-dark-dark solitons (DDD) [13, 47]. For $q = 0$, we obtain exact solutions for finite velocity V :

$$\psi_{0,\pm 1} = \sqrt{n_b^{0,\pm 1}} \left[\sqrt{\frac{1-V^2}{c^2}} \tanh \left[\frac{(x-Vt)}{\xi} \right] + i \frac{V}{c} \right], \quad (\text{S10})$$

where the width $\xi = \hbar/M \sqrt{c^2 - V^2}$, $c = \sqrt{(g_n + g_s)n_b/M}$ is the group velocity of a gap-less low-lying mode at long wave-lengths [12, 18, 19]. For this DDD soliton, the transverse magnetization F_{\perp} coincides with the total number density n (or mass superfluid density) and

$$F_{\perp} = n = n_b \left[\left(1 - \frac{V^2}{c^2} \right) \tanh^2 \frac{x-Vt}{\xi} + \frac{V^2}{c^2} \right]. \quad (\text{S11})$$

The excitation energy of such a soliton reads

$$\delta K^{\text{D}}[n_b, \mu, V^2] = \frac{4\hbar^4}{3(g_n + g_s)M^2\xi^3} - [(g_n + g_s)n_b - \mu]\delta N, \quad (\text{S12})$$

where

$$\delta N = \frac{2\hbar^2}{M(g_n + g_s)\xi} = \frac{2\hbar}{g_n + g_s} \sqrt{\frac{(g_n + g_s)n_b}{M} - V^2}. \quad (\text{S13})$$

Again we find that the spin correction for the DDD soliton

$$\frac{\partial \delta K^{\text{D}}}{\partial n_b(X)} = [\mu(X) - (g_n + g_s)n_b(X)]\xi \quad (\text{S14})$$

vanishes for the Thomas-Fermi density profile Eq. (S3). Hence the equation of motion is

$$M_{\text{in}} \frac{d^2 X}{dt^2} = f_b, \quad (\text{S15})$$

where

$$M_{\text{in}} = 2 \left. \frac{\partial \delta K^{\text{D}}}{\partial V^2} \right|_{n_b=n^{\text{TF}}} = -4\hbar M \frac{\sqrt{\frac{n_b(X)(g_n + g_s)}{M} - V^2}}{g_n + g_s}, \quad (\text{S16})$$

and

$$f_b = -\left. \frac{\partial \delta K_{\text{scalar}}}{\partial \mu(X)} \frac{\partial \mu(X)}{\partial X} \right|_{n_b=n^{\text{TF}}} = \frac{2\hbar}{g_n + g_s} \sqrt{\frac{(g_n + g_s)n_b(X)}{M} - V^2} \frac{\partial U(X)}{\partial X}. \quad (\text{S17})$$

Then the equations of motion for both scalar dark solitons and DDD solitons are identical:

$$M \frac{d^2 X}{dt^2} = -\frac{d\tilde{U}(X)}{dX} = -\frac{1}{2}\omega^2 MX, \quad (\text{S18})$$

which maps to a particle dynamics in an emergent potential $\tilde{U}(X) = (\omega/\sqrt{2})^2 MX^2/2$.

OSCILLATION FREQUENCY AND AMPLITUDE OF A FDS IN A LINEAR POTENTIAL

In the main manuscript, we present the theoretical predictions of the oscillation frequency and the amplitude for a FDS in a hard-wall trapped system superimposed by a linear potential. Here we show the analytical predictions against the spin-1 GPE simulations of their dependence on the quadratic Zeeman energy q (see Fig. S2).

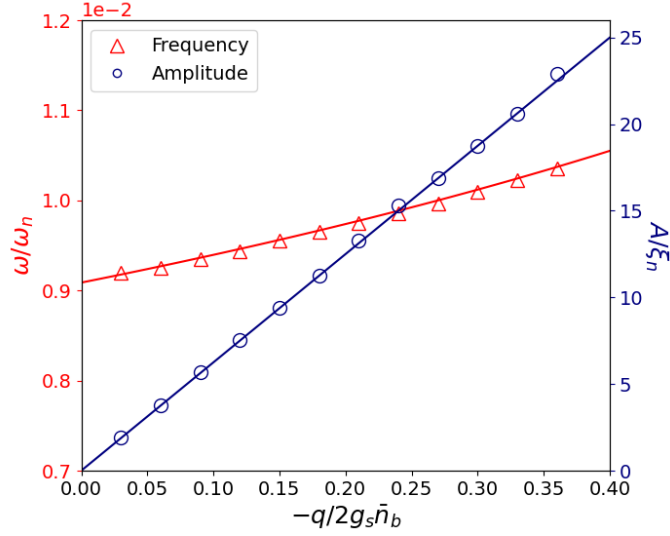


FIG. S2. Comparison between analytical predictions (solid lines) and numerical results (markers) on oscillation frequency and amplitude of a FDS in a linear potential. Here $g_s/g_n = -1/2$, the system size is $200\bar{\xi}_n$, $X_0 = 35\bar{\xi}_n$, $k = 0.008g_n\bar{n}_b/\bar{\xi}_n$, $\mu_N = g_n\bar{n}_b(1 + \bar{q})/2$, $\bar{\xi}_n = \hbar/\sqrt{Mg_n\bar{n}}$, $\omega_n = g_n\bar{n}_b/\hbar$ and \bar{n}_b is the average number density.

SPIN CORRECTIONS FOR MAGNETIC SOLITONS

There exists so-called magnetic solitons in a two-component BEC [9, 30] and the density difference $n_1 - n_2$ has the meaning of spin polarization. Within the formulation presented in the main manuscript, the soliton energy is

$$\delta K(n, \mu, V^2) = n\hbar \sqrt{\alpha \frac{\bar{g}n}{M} - V^2} + (gn - \mu)\delta N \quad (\text{S19})$$

and the depleted atom number

$$\delta N = \frac{3\hbar}{2\bar{g}} \sqrt{c_s^2 - V^2}. \quad (\text{S20})$$

The buoyancy force

$$f_b = -\frac{\partial \delta K}{\partial \mu(X)} \frac{\partial \mu(X)}{\partial X} = \frac{3\hbar}{2\bar{g}} \sqrt{c_s^2 - V^2} \frac{\partial U(X)}{\partial X}, \quad (\text{S21})$$

and the spin correction

$$f_s = -\frac{\partial \delta K}{\partial n(X)} \frac{\partial n(X)}{\partial X} = \frac{\hbar}{2\bar{g}} \frac{V^2}{\sqrt{c_s^2 - V^2}} \frac{\partial U(X)}{\partial X}, \quad (\text{S22})$$

where $c_s = \sqrt{\alpha \bar{g}n/M}$ is the speed of “spin sound”, $\alpha = \delta g/2\bar{g} \ll 1$, $\bar{g} = \sqrt{g_{11}g_{22}}$ and $\delta g = \bar{g} - g_{12}$. Here $g_{11} = g_{22}$ and $g_{12} = g_{21}$ refer to intra- and interspin coupling strength, respectively.

Then the total force reads

$$f = \frac{\hbar}{g} \left(\sqrt{c_s^2 - V^2} + \frac{c_s^2}{2\sqrt{c_s^2 - V^2}} \right) \frac{\partial U(X)}{\partial X}, \quad (\text{S23})$$

which is consistent with Eq. (34) in Ref. [9].